J. Inst. Eng. India Ser. A (December 2019) 100(4):649–657
https://doi.org/10.1007/s40030-019-00393-9

ORIGINAL CONTRIBUTION

# Failure Probability of Structural Systems in the Presence of Imprecise Uncertainties

**S. K. Spoorthi**[1] · **A. S. Balu**[1]

Received: 25 April 2019 / Accepted: 31 July 2019 / Published online: 8 August 2019


**Abstract** Structural reliability evaluation is considered to be the solution for modern complex engineering systems possessing uncertain parameters. Reliability estimation involves probabilistic theory when the uncertainties are defined as random variables, whereas with limited resources, it is strenuous to estimate precise parameters in the structural model. Therefore, for such cases, imprecise parameters should be treated appropriately in the design and analysis stage for the improvement of serviceability of the system. On the other side, analyses involving multi-dimensional, computationally expensive, and highly non-linear structures are formidable in simulation-based methods in the presence of uncertainties. An efficient uncertainty analysis procedure is presented in this paper for analysing the systems with imprecise uncertainties defined as probability-box variables. The estimated bounds of failure probability for the numerical examples from structural mechanics are compared with the traditional approaches to demonstrate the efficiency of the methodology.

**Keywords** Failure probability · HDMR · Imprecise uncertainty · Interval MCS · Probability-box

✉ A. S. Balu
asbalu@nitk.ac.in

S. K. Spoorthi
spoorthi.cv15f11@nitk.edu.in

[1] Department of Civil Engineering, National Institute of Technology Karnataka, Surathkal, India

## Introduction

Uncertainties influencing both structural parameters and imposed loads are important in the prediction of behaviour of the structure. Many approaches have been used to deal with the uncertainties for studying the system responses. These approaches demand a mathematical representation of uncertainties on the basis of available information. Probability theory is the most customary technique to describe uncertainties as random variables characterised by the probability density functions (PDF). If the data are, however, incomplete, ambiguous, and of poor quality, it is difficult to form the PDF. Hence, uncertainty is inadequate to analyse the real structural behaviour by probabilistic theory; therefore, expected structural response may diverge due to the presence of imprecise uncertainties.

Imprecise quantities are defined/expressed as set of possible values that a parameter under consideration varies. Imprecise probability is an extension of traditional probability theory when uncertainties are bounded by lower and upper values for an event. In the past, many researchers considered the uncertainties by representing in many ways based on their sources. For example, evidence theory [1–3], fuzzy sets and possibility theory [4–7], convex models [8–10], Bayesian theory [11–13], interval analysis [14–16], and probability-box (p-box) [17–21] can be found in many engineering applications. The representations are different from one another by the way the incomplete knowledge is interpreted/described mathematically. Also, these theories need the description of variables in bounds rather than precise information about the probability distribution. Structural reliability-based methods were developed with uncertainties; mainly, direct reliability [4–7, 14, 15, 18, 20, 22] and inverse reliability [23–25] are the two methods which were studied and algorithms were

formulated for finding the solution. The lower and upper ranges of structural responses have been extracted by adopting interval finite element method [26]. Matrix decomposition strategy and fixed point formulation were used [19] so as to reduce the overestimation of bounds for uncertain variables, in estimating the structural reliability. Fuzzy [5, 6] and interval [15, 16] parameters are used to quantify the uncertainties with insufficient data in respective studies for the estimation of reliability for complex structures. In the context of imprecise probability, reliability bounds have been evaluated [27], considering imprecise measurements of the members of the structure. To limit the dependency overestimation, interval computation was adopted [28]. Intervals are employed to represent spatial nondeterministic response of structural systems under various loading conditions [22]. Reinforced concrete framed structure was considered for an earthquake loading in the presence of uncertainties in the design of the structure [29]. Probabilistic risk is identified for a retaining wall on considering sensitivity of the variables [30]; also, the study had been extended for the reliability estimation of retaining wall subjected to blast loading with different geotechnical uncertainties [31].

$\underline{P}(E)$ and $\bar{P}(E)$ are a generalised representation of lower and upper probabilities of an event $E$, respectively, with $0 \leq \underline{P}(E) \leq \bar{P}(E) \leq 1$ for any imprecise variable. To handle imprecise uncertainties, interval analysis can be unified with traditional probability theory, called probability bounds analysis, which is generally represented as p-box. It is a general representation of an imprecise variable with lower bound (LB) and upper bound (UB) on its cumulative distribution function (CDF). Computation of reliability index or failure probability becomes burdensome and impractical for the modern multiplex engineering structures. Therefore, simulation methods [e.g. Monte Carlo simulation, (MCS)] and approximate methods like first- and second-order reliability methods (FORM and SORM) are used. These are robust and easy for application, but impractical to generate more samples for real-life examples, in which a complex analysis procedure may be required for the analysis. Hence, for nonlinear systems with more number of uncertainties having imprecise information, traditional simulation-based methods become impractical.

Moreover, design of the system involves repeated analysis to satisfy the design constraints. The complex high-dimensional systems are computationally cumbersome. Hence, approximate models which map the input and output, commonly called response surface methods (RSM), become inevitable. Some of the RSM techniques include sensitivity analysis [11], Kriging meta-models [9, 18], gradient projection method, and Rackwitz–Fiessler algorithms [32]. The application of antecedently mentioned theories is restricted to simple models since they are computationally expensive to adopt for high-dimensional complex structural models. In order to surmount this rigorousness, high-dimensional model representation (HDMR) was introduced by [33]. A concept of support vector regression (SVR) was utilised in computing the sensitivity indices with an adequate number of sample points in accordance with HDMR [34]. The application of HDMR has also been incorporated to uncertainty analysis when the input variables are modelled as interval variables and fuzzy membership functions [5, 6, 14, 34].

The main objective of this work is to propose a methodology for estimating failure probability of structural systems with imprecise uncertainties defined as p-box variables. The HDMR techniques are used for response surface generation, and interval Monte Carlo simulations (IMCSs) are performed for failure probability calculation. The paper is organised as follows. Section 2 presents a brief description of the uncertainties considered and their mathematical operations. Section 3 presents the failure probability assessment and response surface generation in the presence of imprecise uncertainties using HDMR. Both explicit and implicit numerical examples are solved in Sect. 4 to substantiate the proposed methodology. Summary and conclusion are presented in the last section.

## Probability-box (P-box)

P-box approach merges conventional probability theory with the concept of intervals. The p-box gives bounds on CDF for an uncertain variable. Let $x = [\underline{x}, \bar{x}]$ be a p-box, in which $\underline{x}$ and $\bar{x}$ are the LB and UB, respectively. In this paper, the notations followed are as follows: $\mathbf{X}$ for a vector of random variables, $X$ for a random variable, $\mathbf{x}$ for a realisation vector, and $x$ for a realisation of a random variable.

The possible value of $F(x)$ lies in between $\underline{F}(x)$ and $\overline{F}(x)$ for every value of $x$, and it represents the p-box. The expression for failure probability from MCS is given by:

$$P_f \approx \frac{1}{N_s}\sum_{k=1}^{N_s} I[g(x_k) \leq 0] = \left\{ \begin{array}{l} 1, \text{ if } I[\cdot] \text{ is true} \\ 0, \text{ if } I[\cdot] \text{ is false} \end{array} \right\} \quad (1)$$

where $N_s$ is the number of samples, $I[\cdot]$ is the indicator function, and $x_k$ is the $k$th simulated sample of $X$, which can be generated using inverse transform method.

$$x_k = F_X^{-1}(v_j), \quad j = 1, 2, \ldots N \quad (2)$$

where $v_j$ is the sample of random variable. If the variable $X$ is not precisely defined with known PDF, then it may be assumed to fall in between two extreme ranges for the PDF. In this context, failure probability also varies in ranges

$[\underline{P}, \bar{P}]$. This interval of failure probability can be evaluated using IMCS [26] as expressed in Eqs. (3) and (4) which represent bounds of failure probability for all possible values of $F(x)$.

$$\underline{P_f} = \min\left\{\frac{1}{N_s}\sum_{k=1}^{N_s} I\left[g\left(F_X^{-1}(v_j)\right) \le 0\right]\right\} \tag{3}$$

and

$$\bar{P_f} = \max\left\{\frac{1}{N_s}\sum_{k=1}^{N_s} I\left[g\left(F_X^{-1}(v_j)\right) \le 0\right]\right\} \tag{4}$$

Similarly, for $g(\mathbf{x})$, CDF intervals are defined as $\left[\underline{g}, \bar{g}\right]$. The interval bounds are expressed as Eqs. (5) and (6):

$$\underline{g} = \min_{x\in[\underline{x},\bar{x}]}\{g(\mathbf{x})\} \tag{5}$$

and

$$\bar{g} = \max_{x\in[\underline{x},\bar{x}]}\{g(\mathbf{x})\} \tag{6}$$

If $X$ is a Gaussian variable with standard deviation of 0.5, and due to limited resource, mean of the variable is not precise and lies in an interval between [2, 3]; therefore, the variable is modelled as p-box. This imprecise information on the variable is shown in Fig. 1.

## Failure Probability Assessment in the Presence of Imprecise Uncertainties

Failure probability $(P_f)$ is the assessment of the probability of occurrence of an extreme event related to a given structure. In the usual setting, limit state function (LSF) describes the safety level of the structure for a given input vector $\mathbf{X} \in R$. The failure domain (FD), i.e. $F = \{\mathbf{X} \in R | g(\mathbf{X}) \le 0\}$, corresponds to the set of inputs for which the performance function $g(\mathbf{X}) \le 0$.$P_f$ evaluation demands calculation of the probability that the response oversteps a threshold limit, defined by a LSF, mathematically represented as:

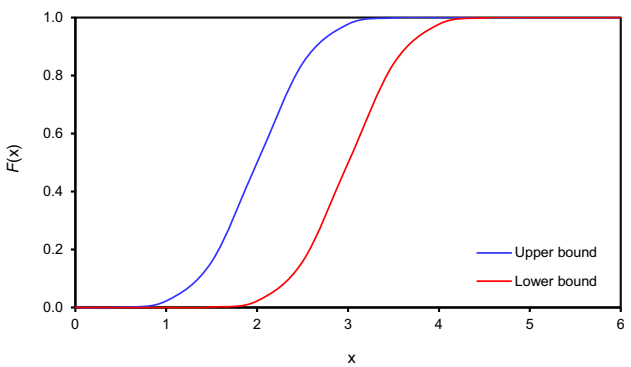


**Fig. 1** P-box with a mean [2, 3] and standard deviation 0.5

$$P_f = P(g(\mathbf{X}) \le 0) = \int_{g(\mathbf{x})\le 0} p_{\mathbf{X}}(\mathbf{x})\mathrm{d}x \tag{7}$$

where $\mathbf{X} = \{X_1, X_2, \ldots, X_N\}$ is the $N$-dimensional vector of random variables of the system under observation; $g(\mathbf{X})$ is the LSF such that $g(\mathbf{X}) \le 0$ represents the FD; and $p_{\mathbf{X}}(\mathbf{x})$ is the joint PDF.

HDMR is a correlated function expansion which maps input–output in an orderly manner. Let $g(\mathbf{X})$ be the response function with $N$ input variables. The first-order HDMR expansion is defined as:

$$\begin{aligned} g(\mathbf{X}) = g_0 &+ \sum_{i=1}^{N} g_i(x_i) + \sum_{1\le i\le j\le N} g_{ij}(x_i, x_j) \\ &+ \sum_{1\le i\le j\le k\le N} g_{ijk}(x_i, x_j, x_k) + \cdots \\ &+ g_{12\ldots N}(x_1, x_2, \ldots, x_N) \end{aligned} \tag{8}$$

where $g_0$ is a constant term representing the response at $\boldsymbol{c}$. Here, $g_i(x_i)$ is a first-order term indicating the effect of $x_i$ acting alone. The function $g_{i_1 i_2}(x_{i_1}, x_{i_2})$ is a second-order term which defines the interdependent effects of the variables $x_{i_1}$ and $x_{i_2}$, and $g_{1\,2,\ldots,N}(x_1, x_2, \ldots, x_N)$ represents any residual dependence of all the input variables which shows the impact on the output $g(\mathbf{X})$.

In contrast to ANOVA–HDMR, which is one of the forms of HDMR, the cut-HDMR specifically exhibits the output in the hyper-plane passing through a reference point $\boldsymbol{c}$ defined in the variable space [14, 33]. After determining each component in Eq. (8), the resulting equation gives HDMR function by replacing the original computationally exorbitant model. The behaviour of the output $g(\mathbf{X})$ is collectively extracted from lower-order correlations up to second order of the input variables [5, 6, 23, 35], by ignoring higher-order terms in Eq. (8). The steps involved for the response surface generation by HDMR are shown in Fig. 2. Here, $N$ and $n$ are number of variables present in the structural system under consideration and number of sample points considered on the variable axes. $\phi_j(x_i)$ is Lagrange's interpolation term for first-order HDMR.

The sampling system for first-order HDMR for a function having one variable $(X)$ and two variables $(X_1$ and $X_2)$ is shown in Fig. 3a, b, respectively.

Based on the previous studies [5, 6, 14, 23, 34, 35], it is witnessed that up to second-order expansions are likely sufficient to characterise outputs of varied realistic systems. In this paper, first-order HDMR expansions are utilised for obtaining $\tilde{g}(\mathbf{X})$ as shown in Fig. 2. For all the values of $N$ and $n$, the function has to be evaluated $N \times (n-1)+1$ number of times for first-order HDMR [35].

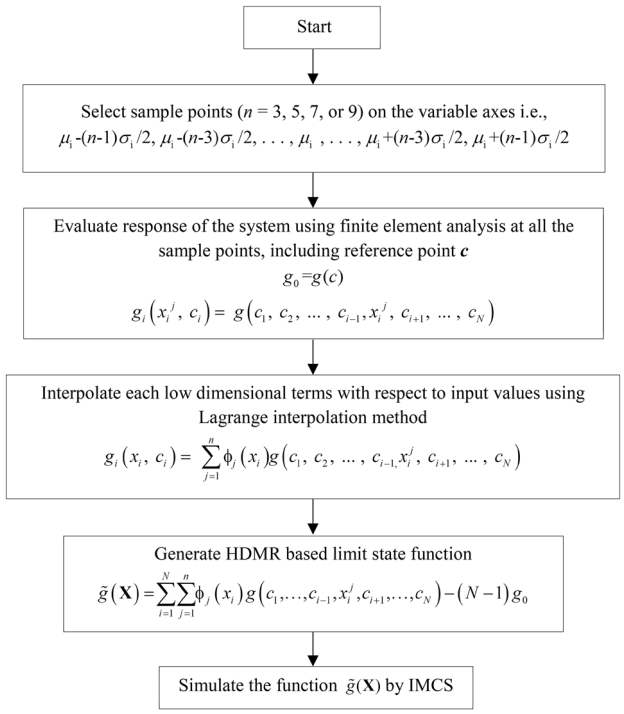


**Fig. 2** Flowchart for generating the first-order HDMR-based function

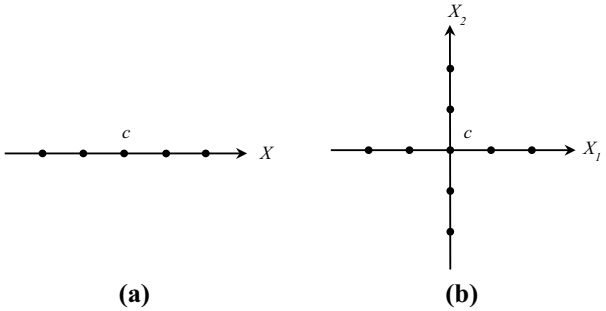


**Fig. 3** Sampling scheme for first-order HDMR: **a** for a function having one variable ($X$) and **b** for a function having two variables ($X_1$ and $X_2$)

## Numerical Examples

In this paper, four numerical examples are illustrated with proposed HDMR-based uncertainty analysis. Both explicit and implicit structural problems are presented to demonstrate the efficiency and applicability of the proposed method. An exact continuous and approximated function obtained from the HDMR technique is simulated with IMCS for different function evaluations, and variation in the bounds of response of the models and failure probability is studied.

### Creep–Fatigue Interaction

A nonlinear creep–failure criterion is considered on the basis of creep and fatigue damage accumulation. The initial explicit model is defined as:

$$g(N_c, N_f, n_c, n_f, \theta_1, \theta_2) = 2 - \exp(\theta_1 D_c) + \frac{\exp(\theta_1) - 2}{\exp(\theta_2) - 1}(\exp(-\theta_2 D_c) - 1) - D_f \quad (9)$$

where $D_c$ and $D_f$ represent the creep damage and fatigue damage, such that, $D_c = n_c/N_c$ and $D_f = n_f/N_f$. $n_c$ and $N_c$ are a number of loading cycles and life of creep, and $n_f$ and $N_f$ are a number of loading cycles and life of fatigue. $\theta_1$ and $\theta_2$ are the experimental parameters. The input parameters are listed in Table 1.

The function in Eq. (9) is analysed using the present method by deploying three samples along each of the variable axis. The original function was evaluated only at the selected sample point locations, and the corresponding component functions are developed; then, the HDMR response function was obtained. The IMCS was applied on the developed HDMR function by simulating the input variables based on their characterisation. In this process, 13 number of function evaluations resulted for the construction of the HDMR function. To study the impreciseness of the failure probability, the CDF was drawn for the LB and UB, as shown in Fig. 4. The function was analysed using other available methods like direct IMCS, FORM, and SORM. Here, the direct IMCS, which requires 500,000 function evaluations, is taken as the reference for the comparison. The proposed technique predicts the failure probability with least computational effort. However, the bounds are wider compared to IMCS. Therefore, the chosen number of sample points along each of the axis was varied from 3 to 7 for seeking improvement in the constructed HDMR model, and the results are presented in Table 2 and Fig. 4. The CDFs for $n = 5$ and $n = 7$ are overlapping exactly with the original function, wherein the pattern of CDFs for $n = 3$ is significantly showing the

**Table 1** Input parameters for creep–fatigue interaction

| Variables | Interval mean | SD |
|---|---|---|
| $N_c$ | [5294,5686] | 549 |
| $N_f$ | [15876,18324] | 3420 |
| $n_c$ | [496,504] | 10 |
| $n_f$ | [11737,12263] | 600 |
| $\theta_1$ | [0.402,0.438] | 0.042 |
| $\theta_2$ | [5.737,6.263] | 0.6 |

deviation, and the curves are wide covering ample of bounds.

### Fracture Strength of Turbine Blade and Disc

The fracture strength of a turbine blade and disc shown in Fig. 5 is considered in this example. The radius of crack of the turbine disc exposed to cyclic loading $N_c$ is defined as:

$$a = \left(\pi^{m/2}(2-m)/2 \cdot c \cdot N_c(2F\sigma_{\max}/\pi)^m + a_0^{1-m/2}\right)^{2/(2-m)} \quad (10)$$

where $c$, $\sigma_{\max}$, and $a_0$ represent the crack propagation, maximum stress, and the radius of initial crack on the surface of the material. The correction factor $F$ and the crack propagation index $m$ are taken as 1.122 and 3.285, respectively. The stress intensity factor for maximum stress near crack tip is defined as $K_{\max} = 2F\sqrt{\pi a}/\pi \cdot \sigma_{\max}$. The LSF is expressed as the difference of critical fracture toughness $K_{IC}$ and stress intensity factor.

$$g = K_{IC} - K_{\max} - 73 \quad (11)$$

The input p-box variables considered for this study are listed in Table 3. Practically, the number of loading cycles $N_c$ can be accurately controlled as a constant in a small amount of the fatigue test; similarly, the crack propagation ($c$) as well as the initial surface crack radius ($a_0$) can also be simply treated as constants when the crack is clear.

The first-order HDMR function is established for the fracture strength of turbine disc by considering $n$ sample points along each of the variable axes, considering $\boldsymbol{c}$ as the mean of p-box variables. Also, the function in Eq. (11) is evaluated using crude IMCS for comparing the computational effort of the HDMR uncertainty analysis which is appreciably lesser than the original function evaluation. Only five function evaluations were required for obtaining the responses, which is computationally very less intensive compared to the direct IMCS (i.e. 500,000 function evaluations). Bounds of failure probability of the function are presented in Table 4, and the corresponding CDFs of the responses are shown in Fig. 6.

**Table 2** Bounds of failure probability of creep–fatigue interaction

| | Failure Probability | | Effort | |
|---|---|---|---|---|
| | UB | UB | LB | UB |
| Direct IMCS | 0.0032 | 0.0039 | 500,000 | 500,000 |
| HDMR ($n$ = 3) | 0.0531 | 0.089 | 13 | 13 |
| HDMR ($n$ = 5) | 0.0033 | 0.0046 | 25 | 25 |
| HDMR ($n$ = 7) | 0.0034 | 0.0051 | 37 | 37 |
| FORM | 0.0093 | 0.0156 | – | – |
| SORM | 0.0178 | 0.0425 | – | – |

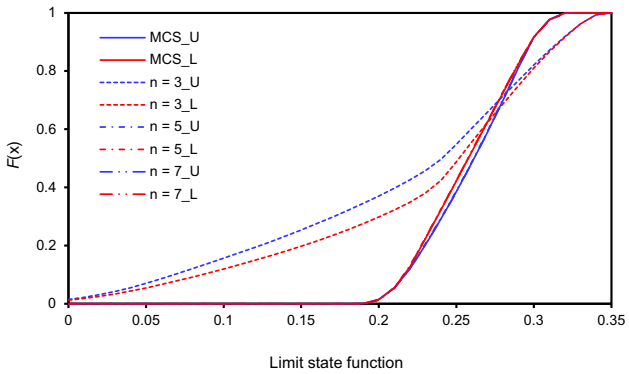


**Fig. 4** CDFs of limit state function of creep–fatigue interaction

Further, $n$ is varied from 3 to 7 to examine the accuracy. It is evident from Table 4 that the failure probability bounds for the LSF obtained using HDMR ($n = 3$) have a slight variation with reference to the original model. However, for $n = 5$, and 7, the CDFs are exact. The effort taken for getting zero error is (nine evaluations) much lesser than that of the direct IMCS. However, as there is no error resulted for the higher values of $n$, the respective bounds are overlapping in Fig. 6.

### Portal Frame

Figure 7 shows the portal frame taken for our study as the implicit problem [35]. The cross-sectional areas $A_1$ and $A_2$ (log-normal) and horizontal load $P$ (normal) are modelled as imprecise uncertainties, and their parameters are given in Table 5.

The values of the second moment of areas are expressed as $I_i = \alpha_i A_i^2 (i = 1, 2; \alpha_1 = 0.08333, \alpha_2 = 0.16670)$. The LSF is defined for deflection in the horizontal direction at the top of the frame.

$$g(A_1, A_2, P) = \Delta_h - \Delta_{\lim} \quad (12)$$

where $\Delta_{\lim} = 6$ mm and $\Delta_h$ is the horizontal deflection. The LSF for the displacement of the portal frame is derived using the first-order HDMR technique by distributing $n$ sample points along each of the variable axis and taking, respectively, the mean values of the p-box variables as reference point $\boldsymbol{c}$.

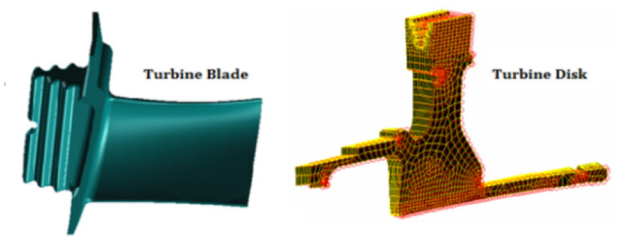


**Fig. 5** Turbine blade and turbine disc

The failure probability is evaluated for all the values of $n$ = 3. Only seven function evaluations were required for obtaining the responses, which is computationally very less intensive compared to the direct IMCS (i.e. 500,000 function evaluations). Bounds of failure probability of the function are presented in Table 6, and the corresponding CDFs of the responses are shown in Fig. 8. Table 6 also presents the bounds of failure probability for sample points $n = 5$ and 7, and FE results by direct IMCS without adopting HDMR for evaluating the efficiency of the methodology. Figure 8 shows CDFs of LSF for different sample points.

The results of the frame for three different variables show the different bounds for all sample points when compared with the direct FE analysis using IMCS without adopting HDMR. From Table 6, for sample points 3 and 5, bounds are nearer; however, $n = 7$ significantly reduces the error with minimum computational effort compared to direct IMCS.

### Plane Truss

A 15-bar steel truss structure [26] is studied with small modification, as shown in Fig. 9. The cross-sectional areas (normal) are $\mathbf{A} = \{A_1, A_2, \ldots, A_{15}\}$, and three loads (log-normal) $\mathbf{P} = \{P_1, P_2, P_3\}$ are considered as p-box variables for the study. First and second moments are listed in Table 7. The LSF is defined for vertical deflection at the node-5 with limit of 0.06 m.

$$g(A_1, A_2, \ldots A_{15}, P_1, P_2, P_3) = \delta_v - \delta_{\text{lim}} \tag{13}$$

where $\delta_{\text{lim}} = 0.06$ m and $\delta_v$ is the vertical deflection obtained by the proposed method. From FE analysis, vertical deflection at node-5 is calculated for all the mean values of variables for deriving the explicit approximated LSF. The failure probability is evaluated for all the values of $n = 3$. As the number of input variables is high compared to other examples, 37 function evaluations were required for obtaining the responses, which is still computationally very less intensive compared to the direct IMCS (i.e. 500,000 function evaluations). Bounds of failure probability of the function are presented in Table 8, and the corresponding CDFs of the responses are shown in Fig. 10.

Similar to the other examples, a parametric study has been carried out for $n = 3$, 5, and 7. Figure 10 shows CDFs of failure probability for the vertical deflection at node-5 for different sample points. The exact ranges are presented in Table 8 as LB and UB, along with the computational efficiency. The errors in the results are compared with that of FE analysis using IMCS. Sample point $n = 7$ is showing more accurate results compared to $n = 3$ and 5.

**Table 3** Input parameters of turbine blade and turbine disc

| Variables | Interval mean | SD |
|---|---|---|
| $\sigma_{\max}$ (MPa) | [655.676,694.324] | 54.0 |
| $K_{IC}$ (kN/m$^{1.5}$) | [83.887,90.113] | 8.7 |

The effort taken for FE analysis with IMCS is way greater than the effort taken for sample point $n = 7$ (i.e. 109).

## Summary and Conclusions

Uncertainties are inherent to most of the physical processes, and therefore, these uncertainties should be quantified efficiently, in which, the characterisation of uncertainty in the input variables is crucial. It is encouraged to consider different kinds of uncertainties in the system, when the information of the uncertainties is imprecise in real-time systems. In this context, a computationally efficient uncertainty analysis method to estimate the failure probability of structural system by modelling the input variables using probability-box is presented in this paper. The behaviour of the system is modelled by the concepts of HDMR, and interval Monte Carlo simulations are implemented to predict the responses in the numerical examples.

Distributions of all the variables are predefined, and no assumptions are introduced in the numerical examples. The proposed method holds good for all kinds of distributions of parameters with inadequate statistical data. The numerical examples, which possess the explicit nonlinear functions, are directly used for simulation; then, the function is approximated using first-order HDMR in which the polynomial-type function replaces the original nonlinear function. The number of sample points in each of the variable axis is varied from 3 to 7 so that the improvement in the accuracy of the approximated HDMR function is witnessed. The simulation of the original nonlinear function over million times is evidently cumbersome as compared to the HDMR-based polynomial function in terms of computation effort. However, in case of implicit examples,

**Table 4** Bounds of failure probability of turbine blade and turbine disc

| | Failure Probability | | Effort | |
|---|---|---|---|---|
| | LB | UB | LB | UB |
| Direct IMCS | 0.0172 | 0.0200 | 500,000 | 500,000 |
| HDMR ($n$ = 3) | 0.0177 | 0.0202 | 5 | 5 |
| HDMR ($n$ = 5) | 0.0174 | 0.0198 | 9 | 9 |
| HDMR ($n$ = 7) | 0.0174 | 0.0197 | 13 | 13 |

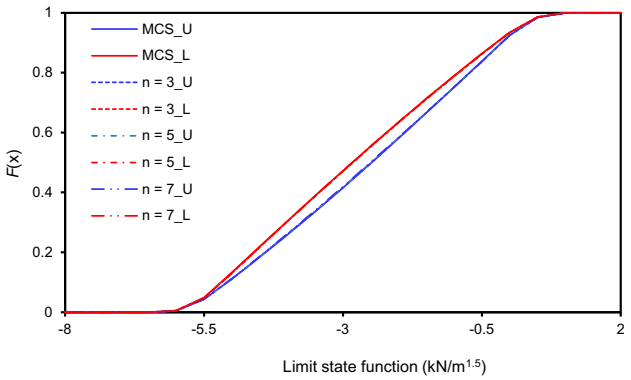


**Fig. 6** CDFs of limit state function of turbine blade and turbine disc

**Table 5** Input parameters for portal frame

| Variables | Distribution | Mean | Std. Dev. |
|---|---|---|---|
| $A_1$ | Log-normal | [0.325, 0.395] | 0.036 |
| $A_2$ | Log-normal | [0.162, 0.198] | 0.018 |
| P | Normal | [15, 25] | 5.0 |

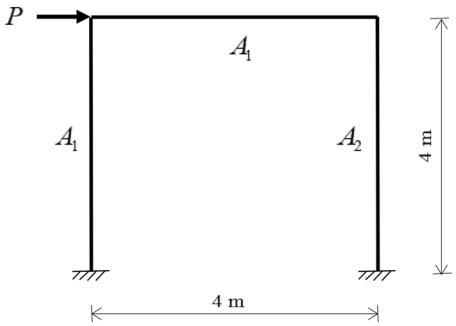


**Fig. 7** Portal frame

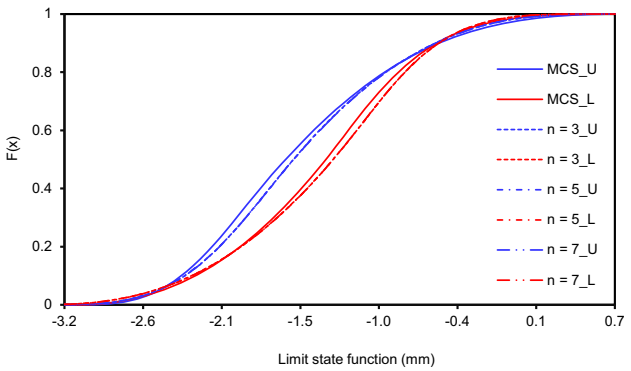


**Fig. 8** CDFs of limit state function of portal frame

**Table 6** Bounds of failure probability of portal frame

| | Failure probability | | Effort | |
|---|---|---|---|---|
| | LB | LB | UB | UB |
| Direct IMCS | 0.0121 | 0.0057 | 500,000 | 500,000 |
| HDMR ($n$ = 3) | 0.0082 | 0.0046 | 7 | 7 |
| HDMR ($n$ = 5) | 0.0082 | 0.0044 | 13 | 13 |
| HDMR ($n$ = 7) | 0.0085 | 0.0046 | 19 | 19 |

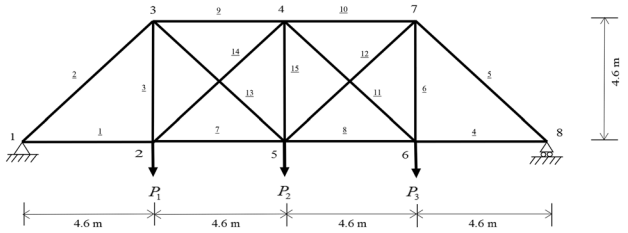


**Fig. 9** Plane truss

**Table 7** Input parameters for plane truss

| Variables | Distribution | Interval mean | SD |
|---|---|---|---|
| $A_1$ to $A_6$ | Normal | [0.001014, 0.001051] | 0.00516 |
| $A_7$ to $A_{15}$ | Normal | [0.000634, 0.000657] | 0.00323 |
| $P_1$ | Log-normal | [84.73, 92.47] | 5.836 |
| $P_2$ | Log-normal | [254.19, 277.44] | 15.839 |
| $P_3$ | Log-normal | [84.73, 92.47] | 5.836 |

**Table 8** Bounds of failure probability of plane truss

| | Failure probability | | Effort | |
|---|---|---|---|---|
| | LB | LB | UB | UB |
| Direct IMCS | 0.0544 | 0.1227 | 500,000 | 500,000 |
| HDMR ($n$ = 3) | 0.0639 | 0.1068 | 37 | 37 |
| HDMR ($n$ = 5) | 0.0669 | 0.1113 | 73 | 73 |
| HDMR ($n$ = 7) | 0.0318 | 0.1247 | 109 | 109 |

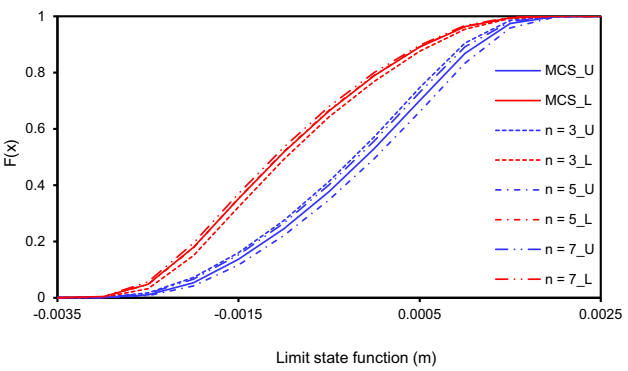


**Fig. 10** CDFs of limit state function of plane truss

the FE analysis carried out for original function evaluation with IMCS is very tedious, as each run takes more time. Therefore, first-order HDMR is adopted to derive the performance function, and the simulation is performed on the HDMR function. The CDFs are presented for all the bounds of the LSF, as the input variables are represented by imprecise probability distributions. In all four examples, the bounds of the failure probabilities obtained from the proposed method are closer to the failure probability bounds of the original model evaluation from the interval Monte Carlo method with lesser effort and high efficiency. In the example of portal frame, it is evident that sample point $n = 7$ shows the lesser percentage of error with the lesser effort of 19 evaluations compared to direct IMCS, whereas in the example of the plane truss, $n = 7$ shows more accurate results as compared to $n = 3$ and 5 with a lesser percentage of error. The effort taken for FE analysis with IMCS (i.e. 5, 00,000) is way greater than the effort taken for $n = 7$ (i.e. 109). From the results obtained using the proposed methodology, the application of HDMR makes the uncertainty quantification more efficient when the imprecise uncertainties are characterised as p-box variables in the systems. It is recommended that the proposed method can be applied to any kind of imprecise uncertainties with less computational effort without compromising on the accuracy.

**Acknowledgements** Not Applicable.

**Funding** Not Applicable.

**Compliance with ethical standards**

**Conflict of Interest** The authors declare that they have no conflict of interest.

## References

1. H.R. Bae, R.V. Grandhi, R. Canfield, A Sensitivity analysis of structural response uncertainty propagation using evidence theory. Struct. Multidisc. Optim. **31**, 270–279 (2006)
2. D.A. Alvarez, J.E. Hurtado, I. Ramírez, Tighter bounds on the probability of failure than those provided by random set theory. Comput. Struct. **189**, 101–113 (2017)
3. T. Feng, S. Zhang, J. Mi, The reduction and fusion of fuzzy covering systems based on the evidence theory. Int. J. Approx. Reason. **53**, 87–103 (2012)
4. S. De, N. Dhang, A literature review on building typology and their failure occurrences. J. Inst. Eng. India Ser. A **100**, 177–190 (2019)
5. A.S. Balu, B.N. Rao, High dimensional model representation based formulations for fuzzy finite element analysis of structures. Finite Elem. Anal. Des. **50**, 217–230 (2012)
6. A.S. Balu, B.N. Rao, Efficient assessment of structural reliability in presence of random and fuzzy uncertainties. ASME J. Mech. Design **136**, 1–11 (2014)
7. S.X. Guo, Z.Z. Lu, A non-probabilistic robust reliability method for analysis and design optimization of structures with uncertain-but-bounded parameters. Appl. Math. Model. **39**, 1985–2002 (2015)
8. A. Zhou, Y. Zhang, Explicit integration scheme for a non-isothermal elastoplastic model with convex and nonconvex subloading surfaces. Comput. Mech. **55**, 943–961 (2015)
9. B. Echard, N. Gayton, M. Lemaire, N. Relun, A combined importance sampling and kriging reliability method for small failure probabilities with time-demanding numerical models. Reliab. Eng. Syst. Saf. **111**, 232–240 (2013)
10. Y. Luo, Z. Kang, Z. Luo, A. Li, Continuum topology optimization with non-probabilistic reliability constraints based on multi-ellipsoid convex model. Struct. Multidisc. Optim. **39**, 297–310 (2009)
11. Z. Hu, S. Mahadevan, D. Ao, Uncertainty aggregation and reduction in structure-material performance prediction. Comput. Mech. **61**, 237–257 (2018)
12. B. Zhu, D.M. Frangopol, Reliability assessment of ship structures using Bayesian updating. Eng. Struct. **56**, 1836–1847 (2013)
13. C. Simon, F. Bicking, Hybrid computation of uncertainty in reliability analysis with p-box and evidential networks. Reliab. Eng. Syst. Saf. **167**, 629–638 (2017)
14. S. Xie, B. Pan, X. Du, High dimensional model representation for hybrid reliability analysis with dependent interval variables constrained within ellipsoids. Struct. Multidisc. Optim. **56**, 1493–1505 (2017)
15. P.R. Adduri, R.C. Penmetsa, Bounds on structural system reliability in the presence of interval variables. Comput. Struct. **85**, 320–329 (2007)
16. O.G. Batarseh, Y. Wang, An interval-based approach to model input uncertainty in M/M/1 simulation. Int. J. Approx. Reason. **95**, 46–61 (2018)
17. H.B. Liu, C. Jiang, J. Liu, J.Z. Mao, Uncertainty propagation analysis using sparse grid technique and saddlepoint approximation based on parameterized p-box representation. Struct. Multidisc. Optim. **59**, 61–74 (2019)
18. R. Schobi, B. Sudret, Structural reliability analysis for p-boxes using multi-level meta-models. Probab. Eng. Mech. **48**, 27–38 (2017)
19. N. Xiao, R.L. Mullen, R.L. Muhanna, Solution of uncertain linear systems of equations with probability-box parameters. Int. J. Reliab. Saf. **12**, 147–165 (2016)
20. X. Liu, Z. Kuang, L. Yin, L. Hu, Structural reliability analysis based on probability and probability box hybrid model. Struct. Saf. **68**, 73–84 (2017)
21. Q. Zhang, Z. Zeng, E. Zio, R. Kang, Probability box as a tool to model and control the effect of epistemic uncertainty in multiple dependent competing failure processes. Appl. Soft Comput. J. **56**, 570–579 (2017)
22. W. Gao, D. Wu, K. Gao, X. Chen, F. Tin-Loi, Structural reliability analysis with imprecise random and interval fields. Appl. Math. Model. **55**, 49–67 (2018)
23. A.S. Balu, B.N. Rao, Inverse structural reliability analysis under mixed uncertainties using high dimensional model representation and fast Fourier transform. Eng. Struct. **37**, 224–234 (2012)
24. J. Lim, B. Lee, I. Lee, Second-order reliability method-based inverse reliability analysis using Hessian update for accurate and efficient reliability-based design optimization. Int. J. Numer. Methods Eng. **100**, 773–792 (2014)
25. I. Lee, K.K. Choi, L. Du, D. Gorsich, Inverse analysis method using MPP-based dimension reduction for reliability-based design optimization of nonlinear and multi-dimensional systems. Comput. Methods Appl. Mech. Engrg. **198**, 14–27 (2008)
26. H. Zhang, R.L. Mullen, R.L. Muhanna, Interval Monte Carlo methods for structural reliability. Struct. Saf. **32**, 183–190 (2010)

27. S. Biswal, A. Ramaswamy, Finite element model updating of concrete structures based on imprecise probability. Mech. Syst. Signal Process. **94**, 165–179 (2017)
28. G. Muscolino, A. Sofi, Analysis of structures with random axial stiffness described by imprecise probability density functions. Comput. Struct. **184**, 1–13 (2017)
29. A. Sil, T. Longmailai, Drift reliability assessment of a four storey frame residential building under seismic loading considering multiple factors. J. Inst. Eng. India Ser. A **98**, 245–256 (2017)
30. A. Guha Ray, D.K. Baidya, Reliability coupled sensitivity based design approach for gravity retaining walls. J. Inst. Eng. India Ser. A **93**, 193–201 (2012)
31. A. Guha Ray, S. Mondal, H.H. Mohiuddin, Reliability analysis of retaining walls subjected to blast loading by finite element approach. J. Inst. Eng. India Ser. A **99**, 95–102 (2018)
32. S.H. Kim, S.W. Na, Response surface method using vector projected sampling points. Struct. Saf. **19**, 3–19 (1997)
33. H. Rabitz, O.F. Aliş, J. Shorter, K. Shim, Efficient input–output model representations. Comput. Phys. Commun. **117**, 11–20 (1999)
34. G. Li, X. Xing, W. Welsh, H. Rabitz, High dimensional model representation constructed by support vector regression I. Independent variables with known probability distributions. J. Math. Chem. **55**, 278–303 (2017)
35. A.S. Balu, B.N. Rao, Confidence bounds on design variables using high-dimensional model representation-based inverse reliability analysis. ASCE J. Struct. Eng. **139**, 985–996 (2013)